DIFFERENTIAL LIGHT SCATTERING FROM SPHERICAL MAMMALIAN CELLS

ALBERT BRUNSTING *and* PAUL F. MULLANEY

From the Biophysics and Instrumentation Group, Los Alamos Scientific Laboratory, University of California, Los Alamos, New Mexico 87544. Dr. Brunsting's present address is the Physics Department, Auburn University, Auburn, Alabama 36830.

ABSTRACT The differential scattered light intensity patterns of spherical mammalian cells were measured with a new photometer which uses high-speed film as the light detector. The scattering objects, interphase and mitotic Chinese hamster ovary cells and HeLa cells, were modeled as (*a*) a coated sphere, accounting for nucleus and cytoplasm, and (*b*) a homogeneous sphere when no cellular nucleus was present. The refractive indices and size distribution of the cells were measured for an accurate comparison of the theoretical model with the light-scattering measurements. The light scattered beyond the forward direction is found to contain information about internal cellular morphology, provided the size distribution of the cells is not too broad.

INTRODUCTION

When a suspension of cells is illuminated by light, it scatters (deflects) this light in all directions. The variation of this scattered light intensity as a function of its direction from the incident direction is called differential scattered light intensity, and the whole process is termed differential light scattering (or DLS). As a means of cell identification, DLS offers certain advantages over traditional methods of light microscopy, i.e., image formation (Cram and Brunsting, 1973). Several studies have indicated that measurements based on scattered light from live cells can establish differences between cell populations not readily observed by microscopic methods (Koch, 1968; Wyatt, 1968; Fiel and Munson, 1970; Wyatt, 1972; Wyatt and Phillips, 1972 *a*, *b*). DLS techniques show potential for being both a rapid and nondestructive probe for unstained live cells. The equivalent depth of the field for DLS measurements presented here is several orders of magnitude larger than that of a microscope with somewhat better resolution. The number of cells producing scattered light in this study is several thousand, producing an averaging effect on the cell population which cannot be achieved easily with light microscopy.

In addition to these advantages for cell suspensions, light-scattering techniques show promise for automated cell analysis (e.g., in flow systems). Leif (1970), Van

Dilla and Fulwyler (1971), and Steinkamp et al. (1973) have discussed potential applications of light scattering in flow systems, while Kamentsky et al. (1965), Mullaney et al. (1969), and Saunders et al. (1971) have used light scattering for cell size measurements or cell size discrimination.

In this study, interphase (G_1) and mitotic (M) Chinese hamster ovary cells (Tjio and Puck, 1958) and HeLa cells in suspension have been studied experimentally and theoretically with DLS methods. We will see that differential scattered light intensity in the forward direction (i.e. the same general direction as the incident light) connotes whole cell size, whereas light scattered at larger angles contains information about internal structure. In addition, if the cell size distribution is too broad, little or no useful information can be obtained from DLS measurements.

A COATED SPHERE MODEL FOR NUCLEATED CELLS

The main scatterer of interest here is the Chinese hamster ovary (CHO) cell which can be modeled morphologically and optically as a coated sphere. The cytoplasm of this mammalian suspension cell is surrounded by a distinct, definite membrane as is its nucleus. For this reason, a coated sphere with its sharp, distinct, optical boundaries was selected as a model. Hopefully, the use of this model (Brunsting, 1972; Brunsting and Mullaney, 1972 *a*, *b*), in comparison to experimental results, will lead to a better understanding of light scattering by mammalian cells. In turn, this may provide us with a new method of cell identification.

In Fig. 1 some representative (Klinger and Hammond, 1971) CHO cells stained with pinacyanol at various times in the life cycle are presented. The photograph of the stained cells does not accurately reflect either the nuclear and plasma membranes or the exact optical properties of the unstained cells; rather, the stain shows the gross morphology at various times in the life cycle.

In the G_1 part of its life cycle just after division, the cell is about 11 μm in diameter (Fig. 1, bottom). As the cell moves through S, when DNA synthesis occurs (Fig. 1, left side), and into G_2 and M just before division (Fig. 1, top and right side), its volume increases to about twice the volume of the G_1 cell or a diameter of about 14 μm. The generation time, or one complete circumscription of the circle in Fig. 1, takes about 17 ± 2 h. The lengths of the labeled sections of arc are proportional to the time spent by the cells in each of their life-cycle parts. The availability of CHO cells, their nearly spherical structure, and their similarity to other interesting mammalian cells make this cell line a worthwhile and practical model system. A cell such as the typical CHO cell will certainly have much greater complexity than the coated sphere model assumed here, but the anticipation is that, as internal details of the mammalian cell change in practice, certain trends in scatter patterns can be predicted and understood with this model.

The assumptions of this model are that both regions, core and coating, are homogeneous and isotropic and can be described by a unique value for the refractive

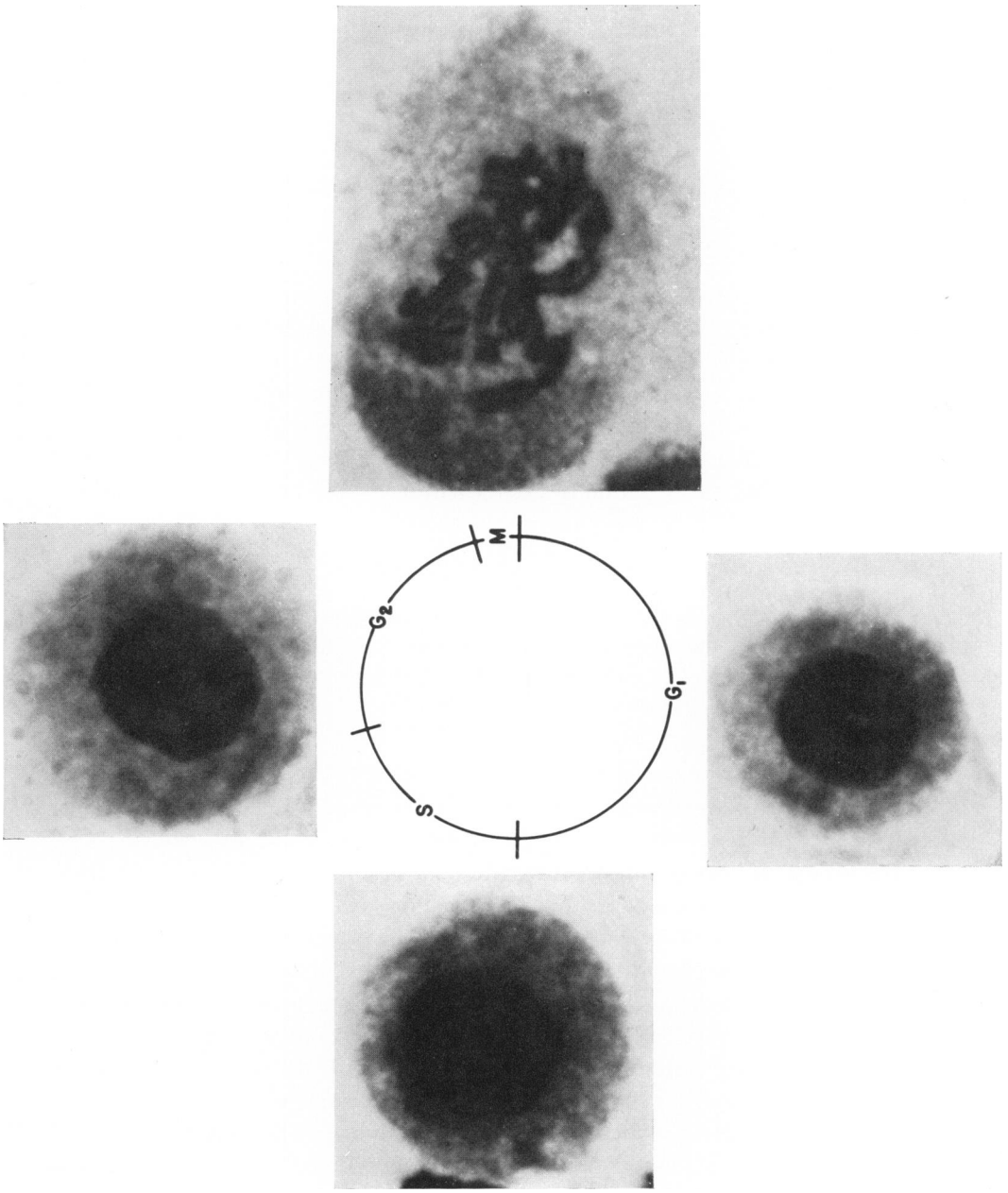

FIGURE 1 Stained CHO cells at various portions of their life cycle (see text for definitions of G_1, S, G_2, and M). Note that cells in M (mitosis) are larger than their daughter cells in G_1 and have chromosomes and no nucleus.

index, possibly complex to account for light absorption. The cell clearly is not homogeneous in its cytoplasm and nucleus and possibly not isotropic, but these regions can be given an effective refractive index (Latimer *et al.*, 1968). Another assumption is that the surrounding medium is isotropic, homogeneous, and nonabsorbing. Finally, Maxwell's equations are used to describe the process. This coated sphere model was first worked out by Aden and Kerker (1951) and by Güttler (1952), who generalized the treatment of Lorenz (1890) and Mie (1908).

DETAILS OF THE PROPOSED MODEL

Let $i_1(\mathbf{x}, \theta)$ represent the differentially scattered light intensity from one cell whose electric field is perpendicular to the scattering plane; $\mathbf{x}$ symbolizes the generalized parameters of the cell based on the coated sphere model (two radii and two relative refractive indices corresponding to the two regions) where θ is the direction of the scattered light ray with respect to the incident beam ($\theta = 180°$ is backscattering). To obtain an average or total intensity pattern for a population of cells at each scattering angle θ, the distribution of each x parameter must be accounted for, i.e.,

$$\bar{i}_1(p, \theta) = \int_{\mathbf{x}-\mathbf{x}_0}^{\mathbf{x}+\mathbf{x}_0} i_1(\mathbf{x}, \theta) p(\mathbf{x})\, d\mathbf{x}. \quad (1)$$

Here $\bar{i}_1$ is the average intensity pattern at θ for a polydispersion of cells, corresponding to the distribution $p(\mathbf{x})$, each one of which has an intensity pattern of $i_1(\mathbf{x}, \theta)$; $\mathbf{x}_0$ is determined so that the multiple integration over $\mathbf{x}$ is negligible outside the limits $\mathbf{x} - \mathbf{x}_0$ to $\mathbf{x} + \mathbf{x}_0$.

For tractable calculations, the experimenter should (*1*) keep the number of integrations as low as possible and (*2*) evaluate the integrand as efficiently as possible. Assuming (*2*) is accomplished, making approximations about $p(\mathbf{x})$ will help with (*1*). It is clear that, to account for the natural variation of G_1 cells, some approximations will have to be made so that the modeling will be solvable.

From Anderson's density work and refractive index measurements discussed below, the assumption is made that the relative refractive indices of the nucleus and cytoplasm, compared to water, are constant and independent of any volume variations. The other assumption is that the nuclear diameter is dependent on whole-cell diameter. To test this, a study was made which attempted to answer the questions, "What is the functional dependence of the two diameters?", and "Is the functional dependence more closely related to diameter or volume?" (i.e., see Kerker, 1969, p. 371). G_1 cells were stained and photomicrographed. This process did not significantly affect their morphology, size, and shape distribution. A visual inspection also revealed no morphological anomalies. Diameters of 21 cells were measured at six angles, 30° apart. The origin of the measurements was chosen to lie at the center of the whole cell. From these six measurements, means and standard deviations for the two diameters can be computed. The result was that $\nu = (1.38 \pm 0.02)\alpha +$

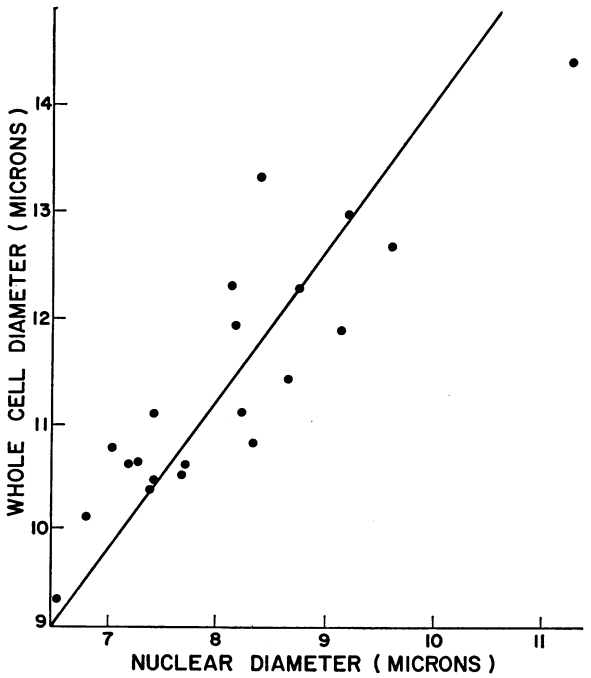

FIGURE 2 Whole-cell diameter versus nuclear cell diameter of CHO cells and a best-fit line.

(0.03±0.05), where α and ν are proportional to the nuclear and whole-cell radii (α and ν are two components of **x**). The data without their respective standard deviations (most of which pass through the best-fit line) are given in Fig. 2.

More parameters certainly could be used to achieve a somewhat better fit of these data, but since departures from the best-fit line are not obvious that approach was not taken. A micrometer scale was photomicrographed and used to size the cells. The average diameters of the nucleus and whole cell were found to be 8.1±0.9 μm and 11.2±0.5 μm, respectively. The uncertainty of these numbers is due mostly to the nonspherical shape of the cell and its nucleus and not to uncertainty in the measurements.

CELL'S RELATIVE REFRACTIVE INDEX AND SIZE

In order to compare theory and experiment, the parameters of CHO cells which are required by theory must be measured. One such parameter is the relative refractive index of the cytoplasm which was measured with phase contrast microscopy (first described by Barer [1955, 1957], Barer and Joseph [1955 *a*, *b*], Barer and Ross [1952], and most recently this technique has been summarized by Ross [1967]). Basically, this method involves immersing one fraction of the cell population in one protein solution and another fraction in another solution, etc. The refractive index of the solutions varies from one to the next. That solution, appearing neither

dark nor bright with respect to the cytoplasm in a phase contrast microscope, has a refractive index closest to the the refractive index of the cytoplasm. The refractive index of the solution is then measured in a refractometer at the wavelength of interest.

Bovine albumin (fraction V, powder, Lot No. 24, Code No. 82-001, from the Research Products Division, Miles Laboratories, Inc., Kankakee, Ill.) was mixed with saline GM (saline G solution is described by Merchant et al. [1960], lacking magnesium and calcium). The physiological saline (saline GM) provides a cell environment in which there is a negligible amount of water crossing its membrane (this effect is discussed below).

At a protein concentration of 26% (i.e., 26 g of bovine albumin to 100 ml of saline GM), the cytoplasm of the cells matched the surrounding solution (discussed above). With a Bausch & Lomb precision refractometer (Model No. 33-45-01; Bausch & Lomb Inc., Rochester, N. Y.), the refractive index of the protein solution was measured to be 1.3703 (the uncertainty to be discussed below). Using the phase technique outlined in Ross (1967, pp. 149 ff), the refractive index of the nucleus was measured to be 1.392 ± 0.005 under these conditions.

What uncertainty can be ascribed to the cytoplasm's relative refractive index, and is the uncertainty biological or instrumental in nature? To answer these questions, let us examine the density invariance of CHO cells around their life cycle and with respect to each other at each stage of their life cycle. Anderson et al. (1970) showed that exponentially growing CHO cells are very homogeneous with respect to density. It was shown that these cells had a coefficient of variation (the standard deviation divided by the mean of the distribution) in density of 0.24% (corresponding to a 5% coefficient of variation in reduced density [i.e. the density minus one]) from one cell to the next and around their life cycle. Barer and Joseph (1954) have shown that the density, d, and relative refractive index, m, of a cell are very closely related by:

$$(m - 1)/d = \text{constant}, \tag{2}$$

where this ratio was very constant over the conditions encountered in this work. It is easy to see, in a general way, why Eq. 2 holds, assuming that the overall velocity of light is reduced by absorption and reemission of photons by the atoms or molecules. Hence, this reduction is proportional to number of atoms or molecules per unit length, or density, and this velocity reduction increases the relative refractive index. Making the assumption that the nuclear density of cells is invariant from one cell to the next, the cytoplasm of CHO cells by Anderson's (1970) work and Eq. 2 has a refractive index of 1.371 and a standard deviation of 0.001. The relative refractive index can be measured with a precision of at least a factor of three times better than this standard deviation; hence, the uncertainty in refractive index arises mostly from the uncertainty in Anderson's density measurements. This standard

deviation is quite accurate and applies to the variation of relative refractive index from one cell to the next and around their life cycle.

The cells were suspended in F-10 growth medium during the light-scattering measurements. It is important to measure the relative swelling or shrinking of the cells in this medium with respect to the 26% bovine albumin solution. Appreciable swelling or shrinking due to water migration across the cell membrane (the dry mass remains constant [Barer and Joseph, 1954]) will cause a difference in refractive index between the two liquids. Any water migration can be inferred from a Coulter counter volume measurement made in comparison to plastic microspheres which do not swell or contract in one or the other of these solutions.

A Coulter counter (1953, U. S. Patent no. 2,565,508) was used to make this measurement. A histogram of the amplitudes of the Coulter pulses was collected in a multichannel analyzer (Van Dilla et al., 1967). Since the pulses are proportional to volume (Gregg and Steidley, 1965; Harvey and Marr, 1966), the histogram reflects size distribution for spheres. These volume measurements were made, and the results are compared in Table I. The normalized cell volume distribution, $p(V)$, described by the cell volume, V, was assumed to be a skewed Gaussian function given by

$$p(V) = \left(\frac{1 - A}{2\pi\sigma}\right) \exp\left[-\frac{1}{2}\left(\frac{V - \bar{V}}{\sigma}\right)^2\right], \tag{3}$$

where

$$A = \frac{S}{2}\left[\left(\frac{V - \bar{V}}{\sigma}\right) - \frac{1}{3}\left(\frac{V - \bar{V}}{\sigma}\right)^3\right]. \tag{4}$$

$\bar{V}$ is the mean volume, σ is the distribution standard deviation, and S is the coefficient of skewness. This distribution was found to fit the Coulter volume distributions better than other distributions such as the zeroth order logarithmic distribution (Espenscheid et al., 1964). The fit was made by taking the histogram data and

TABLE I

COMPARISON OF MICROSPHERES AND RANDOM CHO CELLS IN F-10 MEDIUM AND BOVINE ALBUMIN SOLUTION

	F-10 medium		Bovine albumin solution	
	Cells	Microspheres	Cells	Microspheres
$\bar{V}$	43.5 ± 1.0	34.29 ± 0.04	52.1 ± 0.5	39.49 ± 0.06
σ	9.1 ± 1.1	1.21 ± 0.03	12.9 ± 0.6	3.18 ± 0.06
s	0.3 ± 0.2	0.2 ± 0.10	1.2 ± 0.1	−0.32 ± 0.07

$\bar{V}$, σ, and s are the mean volume signal (Coulter volume spectrometer channel number), standard deviation of V, and coefficient of skewness, respectively.

TABLE II

RESULTS OF A SKEWED GAUSSIAN FUNCTION WITH A CONSTANT BACKGROUND FIT TO THE COULTER VOLUME SPECTROMETER DATA FOR CELLS IN G_1 AND M

Parameter	G_1 cells	M cells
$\bar{V}$	27.97 ± 0.09	57.8 ± 0.10
σ	3.85 ± 0.08	7.3 ± 0.20
s	0.38 ± 0.08	0.44 ± 0.06
b	3.9 ± 0.40	4.7 ± 0.70
$CV = (s/\bar{V}) \times 100\%$	13.7 ± 0.3%	12.6 ± 0.3%

$\bar{V}$, σ, s, b, and CV are the mean volume signal (Coulter volume spectrometer channel number), standard deviation of V, coefficient of skewness, background, and coefficient of variation, respectively.

fitting Eqs. 3 and 4 to them by a nonlinear least-squares algorithm (Moore and Zeigler, 1960). The best-fit parameters, their standard deviations, and a parameter correlation matrix were computed. From the results in Table I, the percentage change in volume of random CHO cells with respect to the plastic microspheres is 3.9± 0.6%. Assuming the dry mass is constant and using Eq. 2, the change in relative refractive index is 0.0013±0.0002 less in bovine albumin than in F-10 medium. When this correction is made, the refractive index of CHO cells in F-10 medium (the scattering solution) becomes 1.372±0.001 with respect to air.

Cells used in the light-scattering measurement were all either in G_1 (with nucleus) or M phase (without nucleus but with mitotic figures), see Fig. 1. The M cells were selected from a monolayer of random CHO cells by a mechanical shake technique (Tobey et al., 1967). After immediate chilling, the drug Colcemid was added to maintain the cells in M phase[1] (Cox and Puck, 1969; Stubblefield and Klevecz, 1965). The G_1 cells were prepared using the technique described above by allowing mitotically selected M cells to divide and grow into early G_1 phase only.

The volume distribution of these two populations of cells was measured with a coaxial flow Coulter volume spectrometer (Steinkamp et al., 1973). These data were then fit with a skewed Gaussian function with a constant background, and the results of that fit are given in Table II. The volume coefficient of variation is slightly larger for G_1 cells than for M cells, which is reasonable since the G_1 population grew from the selected M population (i.e., an extra step). The volume of M cells is about twice that of G_1 cells as determined by mean volumes from Table II—an expected result. The coefficient of skewness is about the same for both populations, as are the matrices of correlation as given in Table III. (A correlation matrix element of ±1.000 in the ith row and jth column implies that, given an elemental increase in the ith [or jth] parameter, the increase [+1.000] or decrease [−1.000] of the jth [or ith] parameter can be predicted with certainty. Moreover, an element of 0.000 in the

[1] Tobey, R. A. Los Alamos Scientific Laboratory, Los Alamos, N. M. Personal communication.

TABLE III

MATRICES OF CORRELATION BETWEEN COMPUTER BEST FITS OF G_1 AND M CELL VOLUME DISTRIBUTIONS

	G_1 cells				M cells			
	$\bar{V}$	σ	s	b	$\bar{V}$	σ	s	b
$\bar{V}$	1.000				1.000			
σ	0.304	1.000			0.473	1.000		
s	0.327	0.086	1.000		0.406	0.161	1.000	
b	−0.092	−0.431	0.092	1.000	−0.346	−0.810	0.073	1.000

The two matrices are symmetric about the diagonal by definition (see text).

*i*th row and *j*th column means that the *i*th [or *j*th] parameter cannot be predicted with any certainty given the *j*th [or *i*th] parameter.) These similarities seem to indicate that most of the cells were synchronized (~95%, Tobey et al., 1967) and divide in the same way.

EXPERIMENTAL MEASUREMENTS

The DLS measurements were made with a photometer using photographic film (Brunsting and Mullaney, 1972 *c*). A 5-mW helium-neon laser provided the incident light, as shown in Fig. 3. The cell suspension (~5 × 10^4 cells/ml) was placed in a cuvette at the center of the photometer, and the differential scattered light intensity was recorded on red-sensitive film (Kodak 2479RAR). Small pins in the film track produced an abbreviated shadow on the film so that the scattering angle, θ, could be determined. Because a rectangular cuvette was used, the measured scattering angle was corrected to account for light refraction at the cuvette-liquid interface. The angular resolution of the photometer is better than 0.5° at θ = 20° and improves to better than 0.05° at θ = 2°.

After film development, the differential scattered light intensity was obtained by reading the film density with a densitometer. The readings were compared with a calibration made for each roll of film. The system has been tested successfully using uniform 10.9-μm diameter polystyrene microspheres (Brunsting and Mullaney, 1972 *c*). The photometer-densitometer system has much greater resolution of DLS intensity versus angle, θ, than is required here.

The measurements were carried out in the θ = 2.5–25° range. There were several reasons for choosing this range. From the calculations on poly-dispersion, most of the DLS intensity lies in the first 20° or so, and there are significant differences between coated and homogeneous spheres in this range. Hence, this is a region of high scattered light intensity with respect to background light scattered and is a promising region to explore. Mullaney et al. (1969) have already studied extensively the small-angle scattering region (θ = 0.5–2.0°) with plastic microspheres and CHO cells. Their results plus the theoretical studies of Hodkinson (1966), Brunsting and Mul-

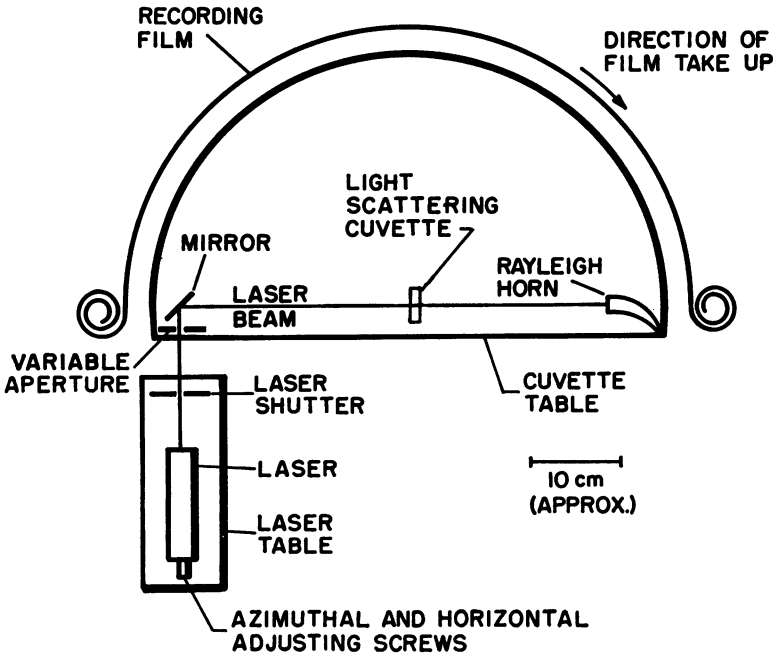

FIGURE 3 Schematic diagram of the film photometer. The laser provides incident light to the scatterers in the cuvette. Most of the laser light is dumped into the Rayleigh horn while the film records the scattered light.

laney (1972 *a*, *b*), and Meehan and Gyberg (1973) imply that small-angle scattering is understood and need not be included in the experimental part of this study (Steinkamp et al., 1973).

Normalization of intensity levels of the experimental curves was chosen so as to match best the corresponding theoretical curves. The small angles empirically were weighted heavier than the larger angles because the small angles had less uncertainty in the intensity measurements.

In Fig. 4, measurements of the DLS patterns are presented along with theoretical predictions for CHO cells in *M* phase. In the range of $2.5° \leq \theta \leq 12°$, the theoretical and experimental scatter patterns do not differ by more than 10%. (The theoretical model used for *M* cells was a homogeneous sphere, since *M* cells do not have a nucleus, see Fig. 1.) However, beyond 12°, the experimental curve deviates more as the scattering angle becomes larger until a maximum spread of 50% is reached at 25°. Beyond 20°, the structure of the theoretical curve washes out, and the plot becomes smoothly decreasing, whereas beyond 16°, the structure of the experimental curve washes out as it becomes smoothly decreasing. This wash-out effect occurs because of the finite distribution of cell size and shape. Clearly, accounting for cell volume distribution is a very important theoretical consideration, as discussed by Wallace and Kratohovil (1970). The general agreement of experi-

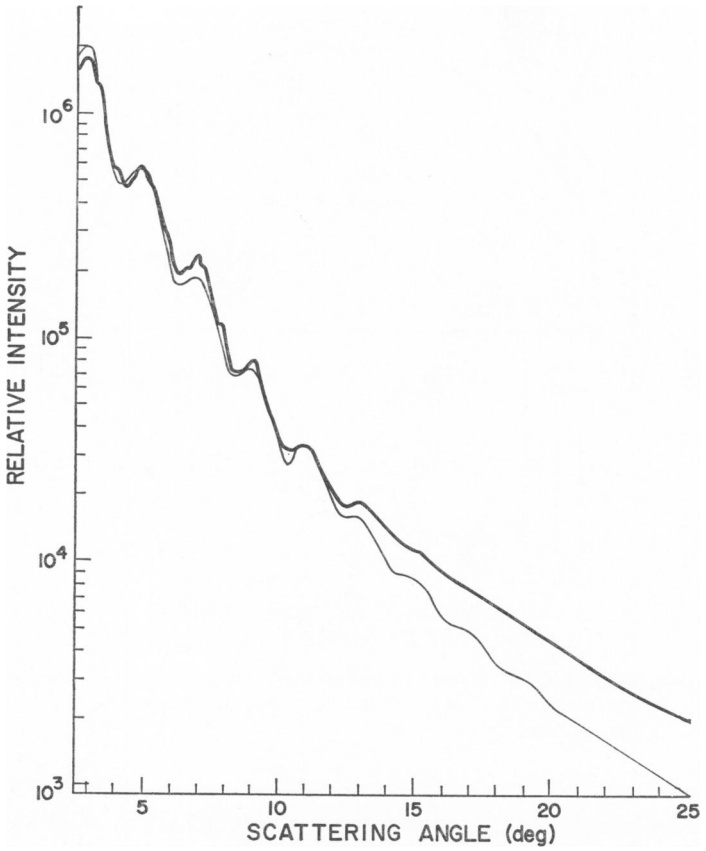

FIGURE 4 A theoretical plot and corresponding experimental results for the differential scatter patterns of CHO cells in *M*. The equivalent homogeneous sphere (thin solid line) and experimental results (thick solid line) are shown.

mental and theoretical curves is quite good, indicating that the measured size distribution was accurate.

For θ between 2.5° and 12.75°, the magnitude of the relative intensity between the two curves lies within two standard deviations (see Brunsting and Mullaney, 1972 *c*). However, beyond 12.75°, departure becomes more acute as the scattering angle increases. This divergency probably can be ascribed to the scatterers in the cuvette. The chromosomes (about 1–8 μm long and 0.5 μm thick) in the nucleus of *M* cells tend to scatter light out to larger angles than the equivalent homogeneous sphere predicts since small objects tend to spread out their DLS patterns more than large objects. The conclusion is that, for θ between 2.5° and 12°, the equivalent homogeneous sphere predicts the *M* cell scatter pattern relatively well but that, beyond about 12°, there is less agreement.

Likewise, there are several observations and conclusions to be made about Fig. 5

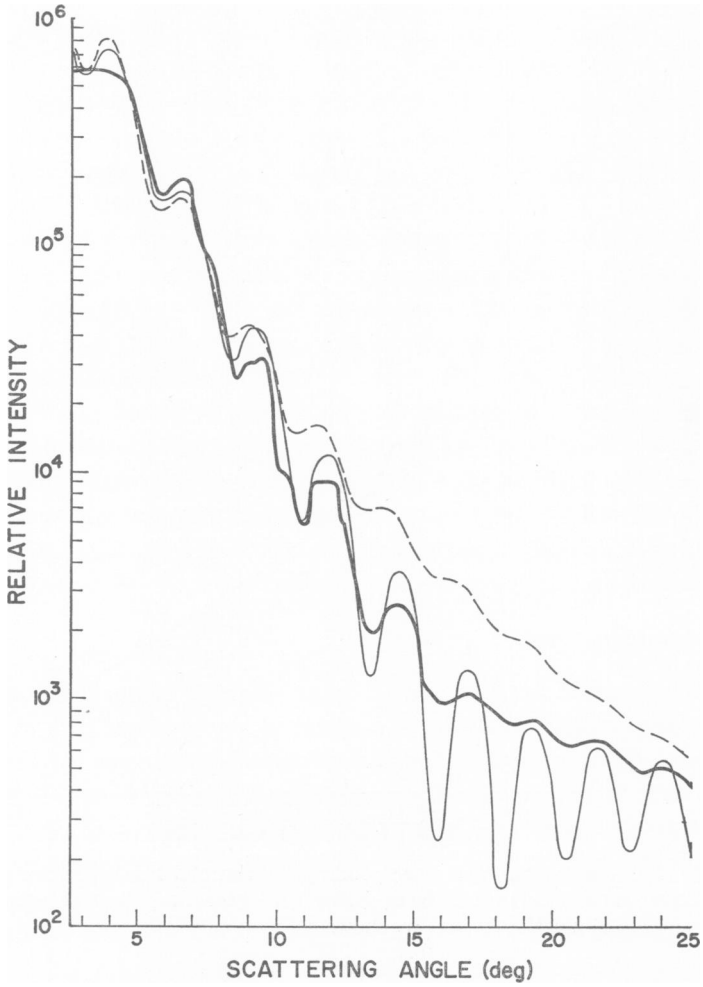

FIGURE 5 Two theoretical plots and corresponding experimental results for the differential scatter patterns of CHO cells in G_1. The coated sphere model (thin solid line), the equivalent homogeneous sphere (thin dashed line) whose refractive index has been volume-averaged from the coated sphere, and the experimental results (thick solid line) are shown.

(CHO cells in G_1). Here the DLS measurements are compared with an equivalent homogeneous sphere (Brunsting and Mullaney, 1972 *c*) and a coated sphere model. In the angular range of 2.5° to about 8.0°, the measurements and theoretical curves track each other within two experimental standard deviations. Beyond 8.0°, the experimental curve departs much more from the equivalent homogeneous sphere curve than from the coated sphere curve. Also, the experimental curve has more fine structure (i.e. ratio of peak-to-valley intensity levels) beyond approximately 10° than the homogeneous sphere would indicate. Moreover, in this angular region, the

location of the extrema of the experimental results agrees much better with the coated sphere model than with the homogeneous sphere model.

Light-scattering measurements were made on HeLa cells which have about 25% more volume than CHO cells and a nucleus with a diameter about 55% of the whole-cell diameter. The coefficients of variation of the volume distributions were found to be $30.6 \pm 1.6\%$ for cells in G_1 (by comparison, see Table II for CHO cells). The same technique was used for synchronizing HeLa cells in M and G_1 as was used for the CHO cells. The DLS measurements indicated no structure in the differential scattering curves, just a smooth three-decade fall-off from 2.5 to 25° in both cases. Little or no information can be obtained from such patterns unless a comparison study is being made (i.e. some parameter of the cell is varied and the corresponding DLS pattern changes). The reasons for this lack of structure may be because the size distribution was too broad (as suggested by computer results), and the refractive index may not have been very constant from cell-to-cell as established in the CHO case. Because the cell system was too ill-defined in terms of size distribution and refractive index, little useful information was obtained from the scattering pattern. These experimental results were predicted theoretically.

CONCLUSIONS

From Fig. 5 we see that the measured differential scatter patterns agree better with the coated sphere model, which takes account of the presence of a nucleus in the cell, compared with the homogeneous sphere model, which was used heretofore to model DLS from large cells. The average levels of intensity from 2.5° to about 16° and from 16 to 25° form two regions of distinctly different slope in the coated sphere calculations and measured patterns. However, the homogeneous sphere calculations do not have two such distinctly different regions. The average intensity of the experimental and coated sphere curves agrees better than the experimental and homogeneous sphere curves beyond about 7°.

The basic conclusion from this work then is that DLS measurements from reasonably concentrically spherical types of cells (or scatterers) which are made outside the first intensity minimum reflect internal structure and permit an estimation of nuclear size to be made (see Fig. 4 of Brunsting and Mullaney, 1972 *b*). If the scatterers are measured one at a time, as in a flow system, then these techniques can be applied and tested with many kinds of spherical cells and particles. On the other hand, if the scatterers are measured in suspension, then the cells must be rather monodisperse in their volume (as in the CHO case and not in the HeLa case) and refractive index distributions. The degree to which the scatterers must have this monodispersity should be determined by the experimenter and is subject to study by the theoretical techniques discussed in past papers (Brunsting and Mullaney, 1972 *a*, *b*, *c*).

This work builds on that of others, in particular that of Berkman et al. (1970),

Fiel (1970), Fiel and Munson (1970), Fiel et al. (1970), Wyatt (1970), and Cross and Latimer (1972). A Coulter volume spectrometer was used to incorporate the cell size distribution in the theoretical treatment. Also, accuate refractive index measurements were used in a new mammalian cell model, the coated sphere. The theoretical treatment was tested against measurements made with a new experimental technique, the film photometer. The results were interpretable in terms of internal structure of the scatterers (CHO cells discussed above and PK-15 cells discussed by Cram and Brunsting [1973]) as well as their size (microspheres, Brunsting and Mullaney [1972 *c*], CHO cells, and PK-15 cells). Therefore, it appears that two properties of cells may permit identification of cell types: gross size (forward scattering) and nuclear size (at angles beyond the forward direction).

We wish to thank several people for their assistance in this work: D. W. Steinhaus (film technology), D. F. Petersen, R. A. Tobey, P. C. Sanders (cell biology), and J. Grilly (microscopic techniques). J. R. Coulter of our Laboratory also helped with the design and fabrication of the photometer. We also appreciate the several discussions we have had with Doctors E. C. Anderson, D. F. Petersen, and M. A. Van Dilla regarding this investigation.

This work was performed under the auspices of the U. S. Atomic Energy Commission while one of us (Brunsting) was an Associated Western Universities, Inc., Predoctoral Fellow at the Los Alamos Scientific Laboratory.

Received for publication 7 August 1973 and in revised form 17 January 1974.

REFERENCES

ADEN, A. L., and M. KERKER. 1951. *J. Appl. Phys.* **22**:1242.
ANDERSON, E. C., D. F. PETERSEN, and R. A. TOBEY. 1970. *Biophys. J.* **10**:630.
BARER, R. 1955. *Research (Lond.).* **8**:341.
BARER, R. 1957. *J. Opt. Soc. Am.* **47**:545.
BARER, R., and S. JOSEPH. 1954. *Q. J. Microsc. Sci.* **95**:399.
BARER, R., and S. JOSEPH. 1955 *a. Q. J. Microsc. Sci.* **96**:1.
BARER, R., and S. JOSEPH. 1955 *b. Q. J. Microsc. Sci.* **96**:423.
BARER, R., and K. F. A. ROSS. 1952. *J. Physiol. (Lond.).* **118**:38P.
BERKMAN, R. M., P. J. WYATT, and D. T. PHILLIPS. 1970. *Nature (Lond.).* **228**:458.
BRUNSTING, A. 1972. Computer Analysis of Differential Light Scattering from Coated Spheres. Los Alamos Scientific Laboratory Report LA-5032. Available from National Technical Information Service, U. S. Department of Commerce, Springfield, Va.
BRUNSTING, A., and P. F. MULLANEY. 1972 *a. Appl. Opt.* **11**:675.
BRUNSTING, A., and P. F. MULLANEY. 1972 *b. J. Colloid Interface Sci.* **39**:492.
BRUNSTING, A., and P. F. MULLANEY. 1972 *c. Rev. Sci. Instrum.* **43**:1514.
COX, D. M., and T. T. PUCK. 1969. *Cytogenetics.* **8**:158.
CRAM, L. S., and A. BRUNSTING. 1973. *Exp. Cell Res.* **78**:209.
CROSS, D. A., and P. LATIMER. 1972. *Appl. Opt.* **11**:1225.
ESPENSCHEID, W. F., M. KERKER, and E. MATIJEVIC. 1964. *J. Phys. Chem.* **68**:3093.
FIEL, R. J. 1970. *Exp. Cell Res.* **59**:413.
FIEL, R. J., E. M. MARK, and B. R. MUNSON. 1970. *Arch. Biochem. Biophys.* **141**:547.
FIEL, D. J., and B. R. MUNSON. 1970. *Exp. Cell Res.* **59**:421.
GREGG, E. C., and K. D. STEIDLEY. 1965. *Biophys. J.* **5**:393.
GÜTTLER, A. 1952. *Ann. Phys. (Leipzig).* **11161**:65.
HARVEY, R. J., and A. G. MARR. 1966. *J. Bacteriol.* **92**:805.
HODKINSON, J. R. 1966. *Appl. Opt.* **5**:839.

KAMENTSKY, L. A., M. R. MELAMED, AND H. DERMAN. 1965. *Science (Wash. D. C.)*. **150**:630.
KERKER, M. 1969. The Scattering of Light and Other Electromagnetic Radiation. Academic Press, Inc., New York.
KLINGER, H. P., and D. O. HAMMOND. 1971. *Stain Technol.* **46**:43.
KOCH, A. L. 1968. *J. Theor. Biol.* **18**:133.
LATIMER, P., D. M. MOORE and F. D. BRYANT. 1968. *J. Theor. Biol.* **21**:348.
LEIF, R. C. 1970. *In* Automated Cell Identification and Cell Sorting. G. L. Wied and G. F. Bahr, editors. Academic Press, Inc., New York. 146.
LORENZ, L. 1890. *Vidensk. Selskab. Skrifter.* **6**:1.
MEEHAN, E. J., and A. E. GYBERG. 1973. *Appl. Opt.* **12**:551.
MERCHANT, D. J., R. H. KAHN, and W. H. MURPHY, JR. 1960. Handbook of Cell and Organ Culture. Burgess Publishing Company, Minneapolis, Minn.
MIE, G. 1908. *Ann. Phys. (Leipzig)*. **25**:377.
MOORE, R. H., and R. K. ZEIGLER. 1960. The Solution of the General Least Squares Problem with Special Reference to High-Speed Computers. Los Alamos Scientific Laboratory Report LA-2361. Available from National Technical Information Service, U. S. Department of Commerce, Springfield, Va.
MULLANEY, P. F., M. A. VAN DILLA, J. R. COULTER, and P. N. DEAN. 1969. *Rev. Sci. Instrum.* **40**:1029.
ROSS, K. F. A. 1967. Phase Contrast and Interference Microscopy for Cell Biologists. Edward Arnold Publishers Ltd., London.
SAUNDERS, A. M., W. GRONER, and J. KUSNETZ. 1971. *In* Advances in Automated Analysis: Technicon International Congress 1970. Technicon Instruments Corp., Tarrytown, N. Y. **1**:20.
STEINKAMP, J. A., M. J. FULWYLER, J. R. COULTER, R. D. HIEBERT, J. L. HORNEY, and P. F. MULLANEY. 1973. *Rev. Sci. Instrum.* **44**:1301.
STUBBLEFIELD, E., and R. KLEVECZ. 1965. *Exp. Cell Res.* **40**:660.
TJIO, J. H., and T. T. PUCK. 1958. *J. Exp. Med.* **108**:259.
TOBEY, R. A., E. C. ANDERSON, and D. F. PETERSEN. 1967. *J. Cell Physiol.* **70**:63.
VAN DILLA, M. A., and M. J. FULWYLER. 1971. *Acta Cytol.* **15**:98.
VAN DILLA, M. A., M. J. FULWYLER, and I. U. BOONE. 1967. *Proc. Soc. Exp. Biol. Med.* **125**:367.
WALLACE, T. P., and J. P. KRATOHOVIL. 1970. *J. Polymer Sci. (Part A-2)*. **8**:1425.
WYATT, P. J. 1968. *Appl. Opt.* **7**:1879.
WYATT, P. J. 1970. *Nature (Lond.)*. **226**:277.
WYATT, P. J. 1972. *J. Colloid Interface Sci.* **39**:479.
WYATT, P. J., and D. T. PHILLIPS. 1972 *a. J. Colloid Interface Sci.* **39**:125.
WYATT, P. J., and D. T. PHILLIPS. 1972 *b. J. Theor. Biol.* **37**:493.